Gas-Solids Flow Behavior: CFB Riser vs. Downer

H. Zhang, W.-X. Huang, and J.-X. Zhu
Dept. of Chemical Engineering, University of Western Ontario, London, Ontario, Canada N6A 5B9

Comparisons are made in a circulating fluidized-bed riser/downer system between a 15.1 m high, 0.10 m ID riser and a 9.3 m high, 0.10 m ID downer, based on the measurements of the radial distributions of the local solids holdups and local particle velocities along the two columns. Although the core-annulus flow structures exist in both the riser and downer, the radial flow structure in the downer differs largely from that in the riser. The radial distributions of solids holdup and particle velocity in the downer are much more uniform than those in the riser, thus ensuring the low back mixing and the narrow particle residence time distribution in the downer. The axial flow structure in the downer is also more uniform than that in the riser. Due to the high particle acceleration and the high particle velocity in the downer, the overall solids holdup is significantly lower than that in the riser. The microflow structure in the downer, characterized by the low intermittency indices, is also more uniform than that in the riser. These key properties of the downer make it a very promising candidate for industrial applications where short reaction times and high product selectivity are required.

Introduction

The cocurrent upflow circulating fluidized-bed (riser) reactors have achieved considerable attention in the past two decades, in both the fields of academic investigations and industrial applications (Berutti et al., 1995; Zhu et al., 1995). As reviewed by Grace (1990), the riser reactors have found many applications including catalytic cracking, ore roasting, polyethylene production, calcination operations and combustion of a wide variety of fuels. Operating either in the fast fluidization regime or in the transported bed regime, the CFB riser reactor has many advantages over the conventional bubbling or turbulent fluidized-bed reactors, such as high gas-solids contact efficiency, high gas and solids throughput, reduced axial dispersion of both gas and solids phases, and so on. On the other hand, CFB riser reactors still suffer from severe solids backmixing, macrosegregations of gas and solids due to the nonuniform gas and solids flow structure in the radial and axial directions, and microaggregations caused by solids clustering. These shortcomings reduce the contact efficiency between the two phases and lead to undesired distribution of products due to reduced selectivity. These disadvantages of the riser reactor result from both gas and solids flowing against gravity (Zhu et al., 1995). Thus, they could be largely overcome in a new type of reactor, the cocurrent downflow circulating fluidized-bed (downer) reactor.

As a novel gas–solids reactor, the cocurrent downflow circulating fluidized-bed (downer) has been drawing more and more attention due to its advantages over the conventional upflow riser reactor. Compared to the riser, the downer exhibits many advantages, as stated by numerous researchers (Wang et al., 1992; Wei and Zhu, 1996; Herbert et al., 1998; Johnston et al., 1999; Zhang et al., 1999; Zhang and Zhu, 2000). These advantages are particularly beneficial to processes where extremely short, but uniform, contact times between gas and solids are required (Zhu et al., 1995; Zhu and Wei, 1996), such as the pyrolysis of liquid and solid wastes (Bassi et al., 1994; Jiao et al., 1998), the fluidized-catalytic cracking (FCC), and residual oil fluidized catalytic cracking (RFCC).

Since the early 1990s, investigations on the hydrodynamics in the downer reactor have been carried out by different research groups (such as Tsinghua University, Petroleum Institute of France, University of Erlangen, and University of Western Ontario). In recent years, very intensive research on the riser/downer systems have been conducted in this laboratory to obtain more and clearer understandings of the hydrodynamics in riser and downer reactors. Based upon the experimental results from both reactors, systematic comparisons on the hydrodynamics between the riser and the downer are presented in this study. The direct comparisons under the

Correspondence concerning this article should be addressed to J-X. Zhu.
W.-X. Huang is visiting from Sichuan University, Chengdu, China.

same operating conditions, with similar distributor designs and with the riser and the downer in the same combined unit, would provide a clearer picture on the similarities and differences, as well as the advantages and shortcomings, of the two reactors.

Experimental Apparatus

The circulating fluidized-bed riser and downer system is shown in Figure 1. It was designed to incorporate both a riser and a downer in the same circulating operation and allow the experimental studies on the riser and the downer to be carried out separately or simultaneously. The riser was 15.1 m in height with 0.1 m ID and the downer was 9.3 m in height with the same ID as the riser. Compared with the experimental setups used by many other researchers, both the riser and the downer columns were much taller, permitting the gas–solids flow to have a longer distance to develop.

The gas distributor at the riser bottom includes a perforated plate and a bundle of nozzles, with 37 tubes of 8 mm ID uniformly installed on the perforated plate. The perforated plate is for auxiliary gas to fluidize the solids from the storage tank, while the nozzles are for the main gas to carry the solids upward. During the operation, solids from the storage tank were first fed into the riser between the nozzles and the perforated plate and were then carried up the riser by the riser main air from the 37 nozzles, to the riser primary cyclone installed at the top of the downer, where solids were separated from the air at an efficiency of greater than 99%. The air exiting the primary cyclone was further cleaned by the secondary and tertiary cyclones before being finally stripped of fine particles in a baghouse filter. At the downer top, solids were redistributed by a gas–solids distributor located below the dipleg of the riser primary cyclone. The solids distributor had a small fluidized bed (held at minimum fluidization) from which particles fell down into the downer through 31 vertically positioned (with triangular pitch) brass tubes (10.7 mm ID, 12.7 mm OD and 0.36 m long). The gas distributor was a plate with 31 holes (16.7 mm ID) located below the solids distributor fluidized bed, but 50.8 mm above

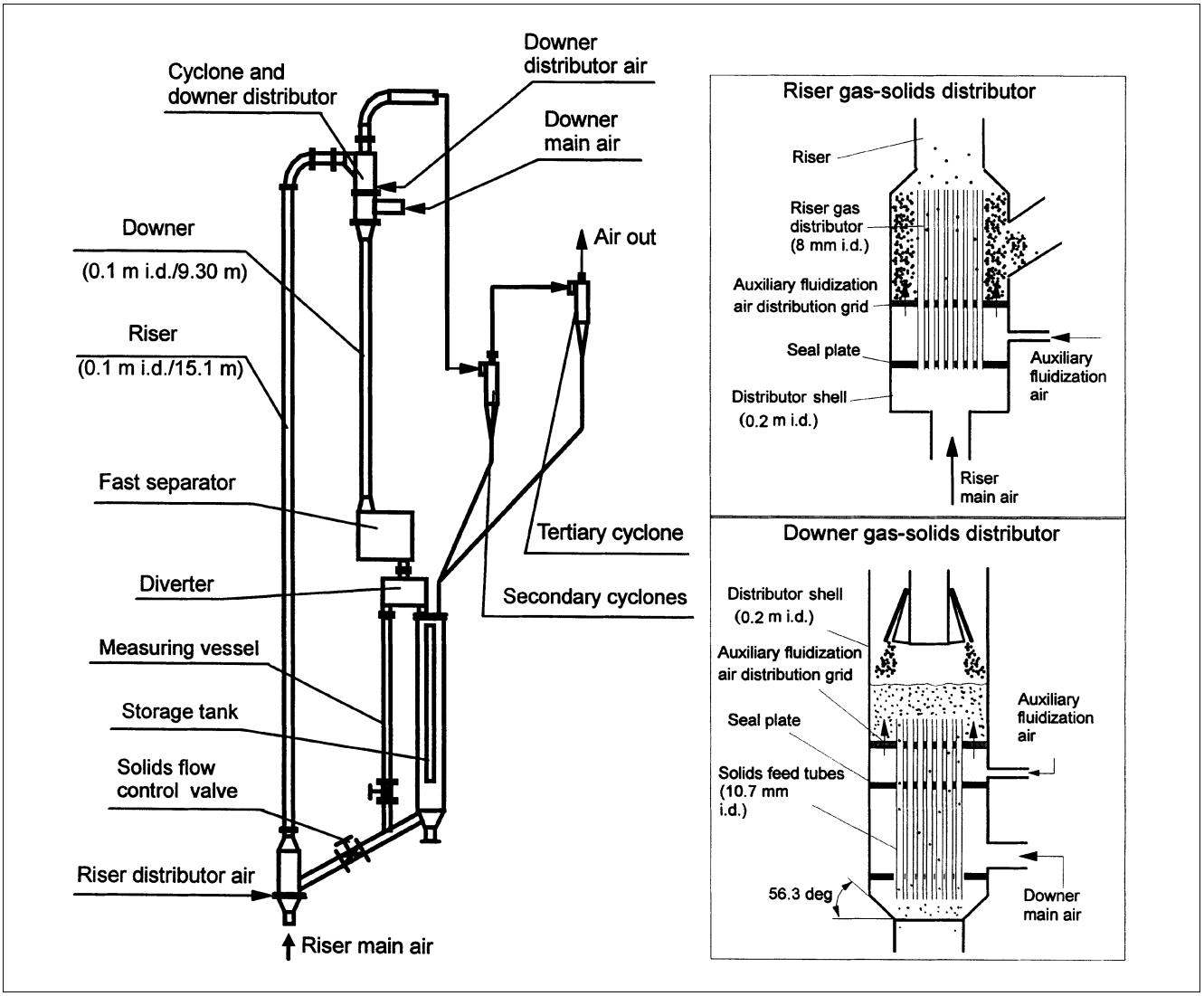

Figure 1. Riser/downer circulating fluidized-bed system.

the bottom exit of the solids feed tubes. Those 31 holes were arranged in the same pattern as the 31 brass tubes in the solids distributor, so that the downer fluidizing gas was distributed through the 2 mm gap between the air holes and the brass tubes, before it begins to contact with downflowing solids from the solids distributor tubes. From the downer entrance, the cocurrent downflow gas-solids suspension traveled down through the downer column. After the exit of the downer, the solids were first separated from the air in a quick inertial separator with an efficiency of more than 99% and then drained to the storage tank. The air was further stripped off the entrained particles by two cyclones before it finally passed through the baghouse. The solids circulation rate was controlled by the solids valve at the riser entrance and was measured by diverting the collected solids from the downer bottom into the measuring vessel for a given period of time.

The particulate materials used for this study were FCC catalyst particles (Sauter-mean diameter = 67 μm, particle density = 1,500 kg/m^3, bulk density = 850 kg/m^3). In order to minimize the electrostatics found in both the riser and downer columns, a small stream of steam was introduced into the main air pipeline to humidify the de-oiled fluidization air to a relative humidity of 70–80%. This has been shown to be very effective. The local solids concentration was measured using an optical fiber solids concentration probe, and the pressure drops along the downer column were measured by a series of pressure transducers. The optical fiber probe for solids concentration had a 3.8 mm OD stainless-steel probe tip, which contains approximately 8,000 emitting and receiving quartz fibers, each 15 μm in diameter. The details of the solids concentration probe have been presented elsewhere (Zhang et al., 1998). The concentration probe was precisely calibrated using a novel calibration procedure, as described by Zhang et al. (1998). The local particle velocity was measured using an optical fiber particle velocity probe. This particle velocity probe had five fibers (two for light emitting, three for light receiving) and a logic circuit to select the correct data and to calculate the particle velocity. The details of the particle velocity probe have been presented by Zhu et al. (2001). The velocity probe was precisely calibrated using a rotating disk device (Zhu et al., 2001). During the experiments, the two probes were alternately inserted into the columns horizontally and moved traversally across the column cross-section. To verify the accuracy of both probes, the local solids flux obtained by multiplying the local solids holdup and particle velocity was integrated over the cross section and compared with the average solids flux (external solids circulation rate), and it was found that the maximum deviation is less than 10% in all locations except for the first 1–2 m at the entrance where the particle flow pattern is still dominated by the distributor effect.

In the riser, six operating conditions were tested. Under each condition, local solids holdups and particle velocities were measured at 11 radial positions on eight axial levels. In the downer, experiments were conducted under 14 different operating conditions (including three zero gas velocity conditions). For each condition, local solids holdup and particle velocities were also measured at 11 radial positions on eight axial levels. Cross-sectional average solids holdups were obtained by integrating the local values at 10 different radial positions excluding the center. Cross-sectional average particle velocities were obtained by integrating the local velocities weighed by the local solids holdups at the same 10 different radial positions.

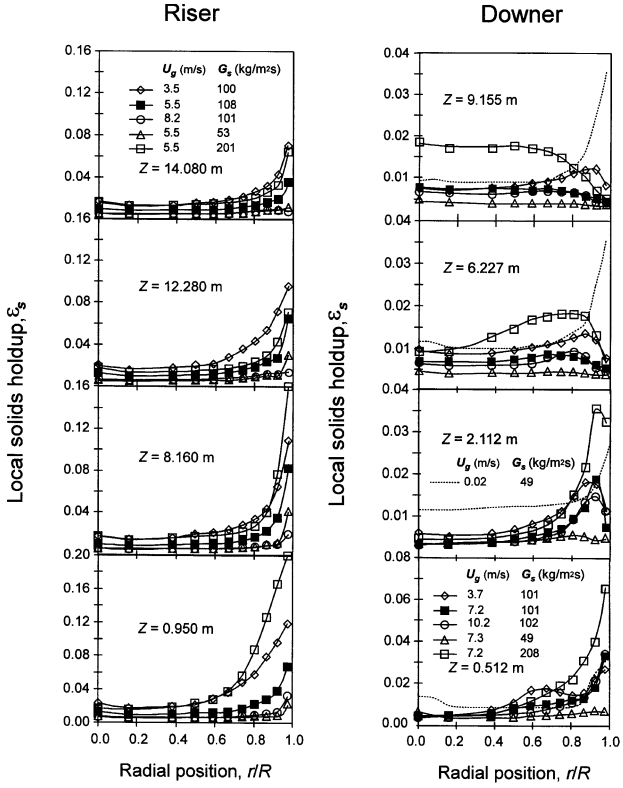

Figure 2. Radial profiles of solids holdup along the riser and downer under different operating conditions.

Results and Discussion

Radial flow structures in the riser and the downer

In order to facilitate the comparisons of the radial gas–solids flow structures between the riser and the downer, the measured radial profiles of solids holdup and particle velocity, the radial nonuniformity indices (Zhu and Manyele, 2001), as well as the intermittency indices (Brereton and Grace, 1993) of the two reactors under different operating conditions, are plotted in pairs in Figures 2 through 5, for four selected axial levels out of the eight levels measured.

Radial profiles of solids holdup. The radial distributions of time-averaged solids holdup in Figure 2 shows distinct differences between the riser and the downer. In the riser, the overall radial structure generally shows a nonuniform solids holdup distribution with a dilute core and a dense annulus, with the radial profile being relatively flat in the core and solids holdup increasing sharply toward the wall in the annulus with the highest solids holdup right at the wall. The radial distribution of solids holdup is affected by the operating condition. It is obvious in Figure 2 that an increase in superficial gas velocity U_g leads to lower local solids holdups across the riser cross-section, lowers the peak of solids holdup at the

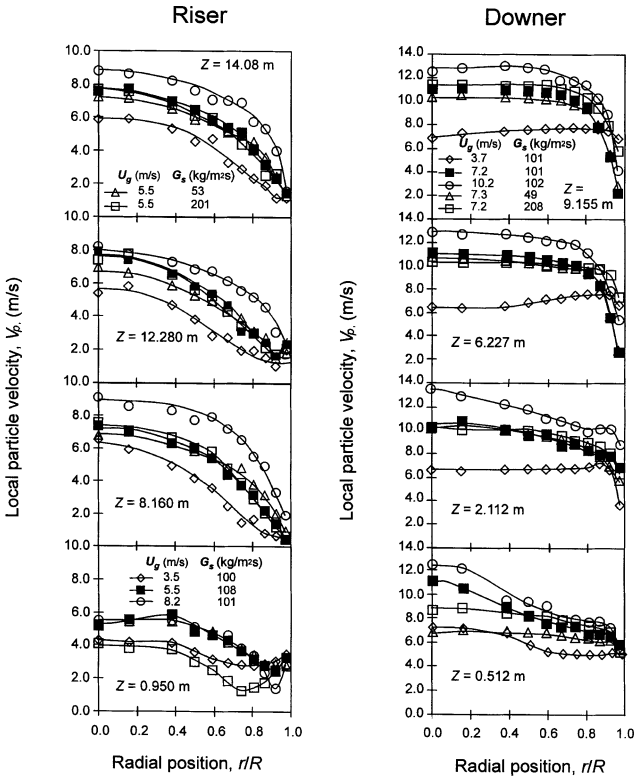

Figure 3. Radial profiles of particle velocity along the riser and downer under different operating conditions.

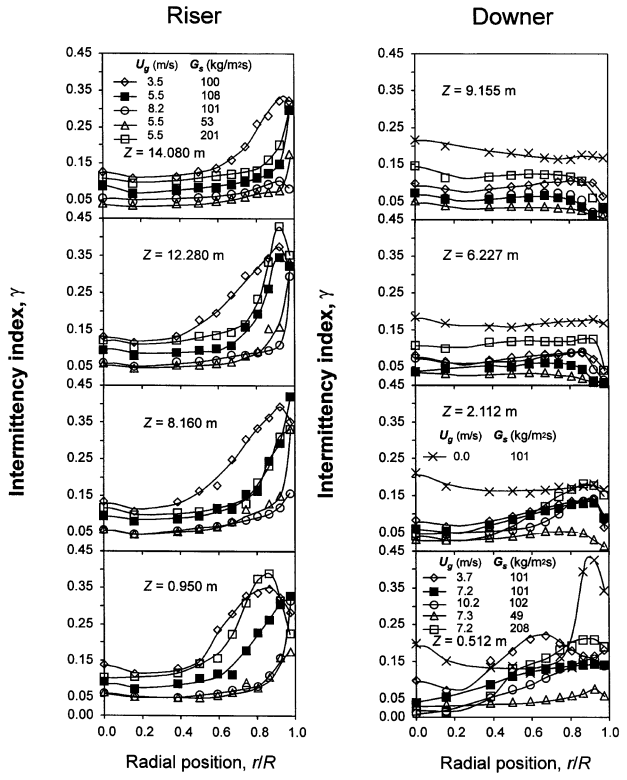

Figure 5. Radial profiles of intermittency indices along the riser and downer under different operating conditions.

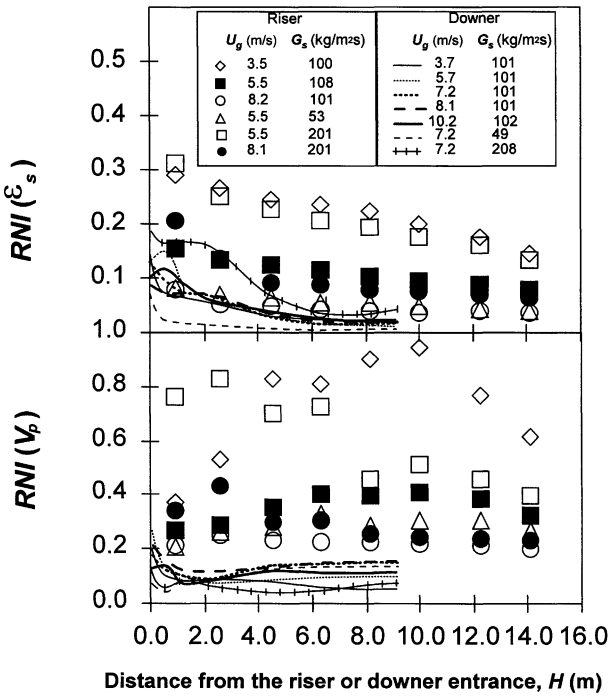

Figure 4. RNI's of solids holdup and particle velocity along the riser and downer under different operating conditions.

wall, and extends the size of the flat core region. An increase in G_s results in an opposite effect, leading to higher local solids holdups across the riser cross-section, a higher peak of solids holdup at the wall and a reduced flat core region. Generally, the radial distributions of solids holdup become more uniform as Z increases. The above findings are consistent with those reported in the literature (Zhang et al., 1991; Berutti et al., 1995).

On the downer side, the overall solids holdup is much lower than that in the riser under comparable operating conditions. This is not surprising because the particles travel down the downer column in the same direction as gravity, which imposes extra acceleration on the particles in the acceleration section and allows the particles to travel faster than the gas in the accelerated section. The overall radial structure in the downer also exhibits a nonuniform radial distribution of solids holdup with, again, a core-annulus structure. Yet, some important differences from that in the riser can be noticed.

First of all, the radial distribution of solids holdup in the downer is much more uniform than that in the riser, as seen from the profiles (note the different scales for the riser and the downer). Secondly, as identified by Zhang (1999), there are two general core-annulus structures in the developed zone in the downer: the dilute core-dense annulus structure at lower gas velocity of less than 4 m/s and the dilute annulus-dense core structure at higher gas velocity of more than 5 m/s. Under low gas velocities, the annular region is signifi-

cantly denser than the core region. As shown in Figure 2, the solids holdup in the annulus, unlike that in the dilute and uniform core, increases toward the wall when U_g is close to zero, or it first increases and then decreases toward the wall with the highest solids holdup (peak) present at $r/R = 0.85-0.90$ when U_g is 3.7 m/s. In other words, the pattern of radial solids holdup distribution with zero U_g is similar to that in the riser, and an increase in U_g from zero to 3.7 m/s starts to break this pattern causing the solids holdup in a small region at the wall to drop. When the superficial gas velocity is higher than 5.7 m/s, the dilute annulus-dense core structure shows up where the solids holdup in the annulus decreases toward the wall, leading to a lean annular region compared to the dense, but uniform, core region. This structure is completely different from that in the riser. Zhang (1999) regarded the above two different structures as two regimes: the dilute core-dense annulus flow regime and the dilute annulus-dense core flow regime.

Our results on the radial profiles of solids holdups are similar to those reported by the Tsinghua University research group (such as Bai et al., 1991a; Wang et al., 1992) and the University Erlangen-Nürnberg research group (Wirth et al., 1998; Lehner et al., 1999), which both show rather uniform radial profiles. One small difference is that they consistently observed a small peak near the wall, while we only observed the same in the middle developing portion of the downer. This could be due to the fact that our downer is much longer and the flow in the other downers may not have been fully developed at the measurement points. On the other hand, the results by Cao and Weinstein (1998) showed extremely nonuniform radial profiles with high solids concentration near the wall. This is not surprising since their data were taken at $Z = 2.50$ and 3.55 m, very close to the distributor, where our data and other data also showed high solids concentration near the wall because of the flow development.

In the downer, the radial solids holdup distribution is influenced by the operating conditions in a different way. Within the dilute core-dense annulus flow regime, an increase in U_g from zero to 5.7 m/s has a major effect on the shape of the radial solids holdup profiles as described above. In the dilute annulus-dense core flow regime, an increase in U_g from 5.7 m/s to 10.2 m/s, the highest U_g tested in this study, has only a minor influence on these profiles, which leads to lower local solids holdups across the downer cross section, but does not change the shape of the radial solids holdup profiles. An increase in G_s has no significant effect on the shape of the radial solids holdup profiles, although it makes the denser region denser in both regimes (see also Zhang et al., 1999; Zhang, 1999, for more profiles). While in the riser, as mentioned earlier, an increase in U_g always lowers the peak of the solids holdup profile and makes the profile more flat, and the effect of an increase in G_s is simply opposite to that of an increase in U_g.

In the downer, the radial distributions of solids holdup become more uniform as the distance from the entrance Z increases. This is similar to the trend in the riser if the exit effect in the riser is not considered. No distinctive exit effect was observed in the downer.

Radial Profiles of Particle Velocity. The radial profiles of time-averaged local particle velocity in the riser and the downer under a variety of operating conditions are plotted in Figure 3. In the riser, the overall radial structure in terms of the particle velocity also shows a core-annulus style where the particles move faster in the core, slower in the annulus with the highest velocity at the center. Normally, the local particle velocity decreases monotonically from the center toward the wall, except for a slight increase near the wall in the entrance section for all operating conditions (or even in higher sections for low U_g conditions). Because of the large amount of downflowing particles in a region adjacent to the wall, it has been reported by many researchers that the local particle velocity in this region could be negative under certain operating conditions, which causes internal circulation of particles. According to their results, this negative local particle velocity is more likely to be present in the bottom section of the riser and, a higher G_s or a lower U_g tends to intensify the internal circulation. However, due to the nozzle type design of the riser gas distributor in this study, the particles entering the riser bottom are entrained upward by the nozzle jets that are uniformly distributed across the whole crosssection, so that the downward average particle velocities were seldom observed in this study. Although, significant particle downflow was observed in the annulus under certain conditions, the average particle velocity is mostly upward.

In the riser, the influence of operating conditions on the radial distribution of particle velocity is simple and monotonous. An increase in U_g largely increases the local particle velocity in the core region, but only increases the particle velocity in the annular region to a small extent, leading to a less uniform radial distribution in the fully developed zone. An increase in G_s does not significantly affect the radial distribution of particle velocity.

It is interesting that, as the particles move away from the riser entrance, the radial distribution of particle velocity normally becomes less uniform (except for those under high G_s conditions), because the difference between the core region and the annular region becomes larger. This is likely caused by the friction between the wall and the gas-solids flow, which slows down the particles in the annulus.

Compared to that in the riser, the radial distribution of particle velocity in the downer is more uniform, although a core-annulus structure is also present. This is mainly due to the existence of the large uniform core region, which covers most of the cross-sectional area in the downer ($r/R \leq 0.75-0.90$). No negative local average particle velocity was observed in the downer.

The effects of operating conditions on the radial profiles of particle velocities in the downer are similar to that in the riser. In the downer, an increase in U_g largely increases the local particle velocity in the core region but only increases the local particle velocity in the annular region by a small fraction, leading to a less uniform radial distribution. An increase in G_s does not significantly affect the radial distribution of particle velocity in the fully developed zone, although it slightly increases the local particle velocity across the cross section.

It is also worth pointing out that in the downer, the radial distribution of particle velocity becomes more uniform down the column (different from that in the riser), because a large uniform core region is eventually formed. No distinctive exit effect was observed in this study, because there is no exit restriction on the downer side.

Radial Nonuniformity Indices. In order to further the analyses on the radial uniformities of solids holdup and particle velocity in the riser and the downer on a quantitative basis, the radial nonuniformity indices (RNI) proposed by Zhu and Manyele (2001) are adopted to compare the radial uniformities of the gas-solids flow between the two reactors. This index is defined for each given parameter as the standard deviation of its values in the radial direction, normalized by the maximum possible standard deviation for the same parameter with the same average cross-sectional value (Zhu and Manyele, 2001). Figure 4 shows the RNIs (RNI(ϵ_s) in terms of the solids holdup and RNI(V_p) in terms of the particle velocity) along the axial directions in both reactors. Great differences in RNIs between the riser and the downer can be seen from the charts, where both RNI(ϵ_s) and RNI(V_p) in the riser are normally several times higher than those in the downer. This reconfirms the earlier observation that the radial flow structure in the downer is much more uniform than that in the riser. Furthermore, RNI(V_p) in the riser does not decrease, and even increases under lower U_g conditions along the axial direction.

The uniform radial distributions of solids holdup and particle velocity in the downer would minimize the difference in the residence times of different particles and would be favorable to a narrow RTD, as has been verified by Wei et al. (1994).

Radial Profiles of Intermittency Indices. The microflow structure in fluid-solids systems can be characterized using several methods, such as the standard deviations of local solids holdup (Brereton and Grace, 1993), the probability density function (Hartge et al., 1988, and Herb et al., 1989) and the intermittency index (Brereton and Grace, 1993), and so on. In this study, the intermittency index is used to compare the time variations of solids holdup between the riser and the downer. A higher intermittency index represents a more segregated flow. Figure 5 plots the radial distributions of intermittency indices in the riser and the downer under a variety of operating conditions. The profiles show that in the riser, the intermittency index is low in the core region and extremely high in the annular region, indicating significantly increased flow fluctuation in the annulus. This pattern remains almost the same throughout the whole length of the riser. The intermittency index increases with increasing G_s or decreasing U_g in both the development zone and the fully developed zone. This suggests increased flow fluctuation with the increase of G_s or the decrease of U_g.

In the downer, the intermittency index near the entrance is low in the core region and high in the annular region, similar to the trend in the riser, although the local values in given radial positions (including the peak value) are lower than those in the riser. However, the peak value quickly decreases and the values in the core region slightly increases as the distance from the entrance increases, leading to a uniform radial distribution of intermittency index across the majority of the radius and a low intermittency index near the wall. In the fully developed zone, the intermittency index increases with increasing solids circulation rate. Hence, the influence of G_s on the intermittency index is similar to that in the riser. On the other hand, the superficial gas velocity affects the intermittency index in a more complex way. An increase in U_g from zero to 7.2 m/s significantly brings it down, while a further increase in U_g from 7.2 to 10.2 m/s on the contrary slightly enhances it. In the fully developed zone in the downer, the intermittency index in the core region is comparable to that in the same region in the riser. In the annular region, it is much smaller than that in the riser. Thus, the microflow structure in the annular region of the downer is much more uniform compared to the riser. In other words, the solids particles in the riser are in a more aggregated form in the annular region, while in the downer, they tend to be in a more particulate form in this region. In addition, the fact that the entire downer is in a more dispersed particulate flow state is in line with the conclusion by Wei and Zhu (1996) from solids dispersion study that the microflow structure in the entire downer resembles that in the core of the riser, where few particles flow through in the form of clusters. Thus, one key advantage of the downer is that the nearly ideal uniform gas-solids suspension, only existing in the core of the riser, can be obtained across the whole downer crosssection.

Development of the gas-solids radial flow structure

The length-of-flow development (LOD) in this study is defined as the comprehensive length that is needed for both the radial solids holdup profiles and the radial particle velocity profiles to become fully developed. To facilitate a detailed comparison, the flow development in each of the core and annulus regions are first separately examined, although the concept of separate flow development in each region may not have any practical meaning. Figure 6 provides a comparison of LODs between the riser and the downer. The figure shows that the length of flow development in the annular region of the downer is comparable to that in the same region of the riser. In the core region of the downer, the length of flow development is always longer than that in the core region of the riser. However, the total length-of-flow development in the downer, which is the longer one of the LOD in the core and the LOD in the annulus, is again comparable to that in the riser. In both reactors, LOD is extended with increasing G_s and decreasing U_g in both the core region and the annular region.

It is worth pointing out that the radial distributions of solids holdup and particle velocity in the development zone of the downer are much more uniform than those in the development zone or even in the developed zone of the riser. Thus, compared to those in the riser, the length of radial flow development becomes a less important parameter in the downer reactor design.

Axial flow structures in the riser and the downer

In the riser, the solids particles are entrained up the column, against gravity, by the upflowing gas flow. In the downer, both the gas phase and the solids phase are flowing downward, in the same direction as gravity, where the solids are accelerated by both gravity and the drag force of the gas phase in the acceleration section. Also, the force of gravity in the downer causes the particle phase to flow faster than the gas phase in the developed section. This makes the axial flow structure in the downer different from that in the riser.

Axial Profiles of Solids Holdup and Particle Velocity. Figures 7 and 8 show the axial profiles of the cross-sectional

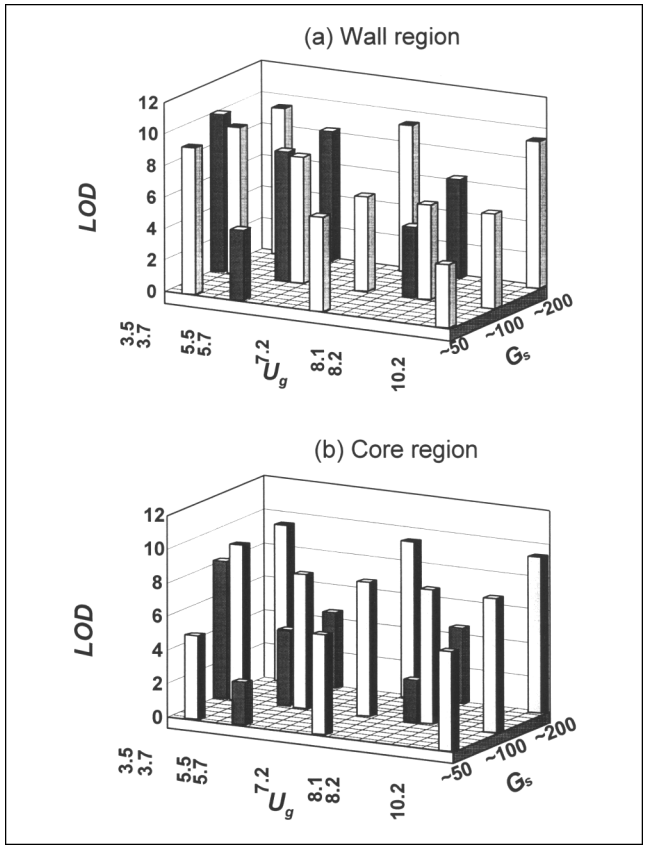

Figure 6. Effects of solids circulation rate and superficial gas velocity on the lengths of radial flow development for the riser and the downer.

(a) in the wall region ($r/R > 0.775$), and (b) in the core region ($r/R < 0.775$). The white columns represent LODs of the downer; the black columns represent the LODs of the riser. Shaded top indicates that LOD is longer than the length of the downer.

average solids holdup and particle velocity measured in the riser and the downer, under a wide range of operating conditions tested in this study. Because of the opposite effects of gravity on the particle phases in the two reactors, the particle velocity in the downer is much higher than that in the riser. This leads to a much lower solids holdup in the downer compared to that in the riser. For all the operating conditions tested (if the entrance section is not considered), the cross-sectional average solids holdup in the downer ranges from 0.005 to 0.02, while under comparable conditions, the cross-sectional average solids holdup in the riser is much higher, showing values between 0.008 to 0.06. Such low solids holdup could be a significant disadvantage of the downer for certain reactions where the requested solids-to-gas ratio is high.

In this study, the high velocity gas jets from the nozzle type riser gas distributor exert a strong drag on the particles so that a dense bed was not formed at the bottom of the riser, although some other researchers have reported the existence of the dense bed under some of the operating conditions used here (Li and Kwauk, 1980; Hartge et al., 1986; Mori et al., 1992). Thus, for all the operating conditions tested in the riser, there exist only two axial sections: the acceleration section

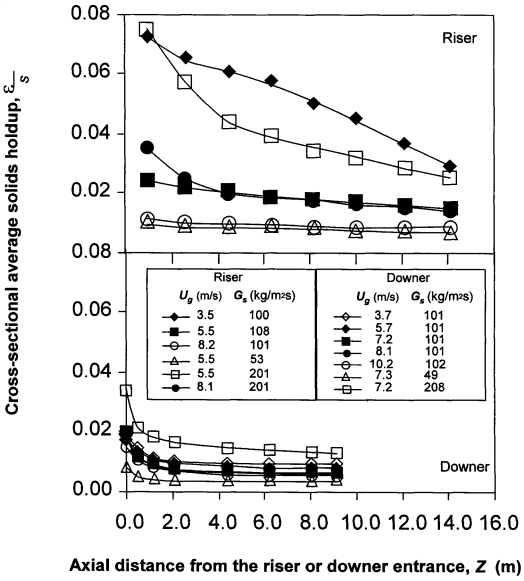

Figure 7. Axial profiles of cross-sectional average solids holdup along the riser and downer at various operating conditions.

where the solids holdup decreases in the axial direction and the constant velocity section where the solids holdup remains constant throughout the rest of the column length. While in the downer, there are three axial sections as described by Wang et al. (1992): the first and second acceleration sections and the constant velocity section.

The profiles in Figures 7 and 8 show that the particle acceleration in the downer is normally faster than that in the riser. For most of the operating conditions tested, the length

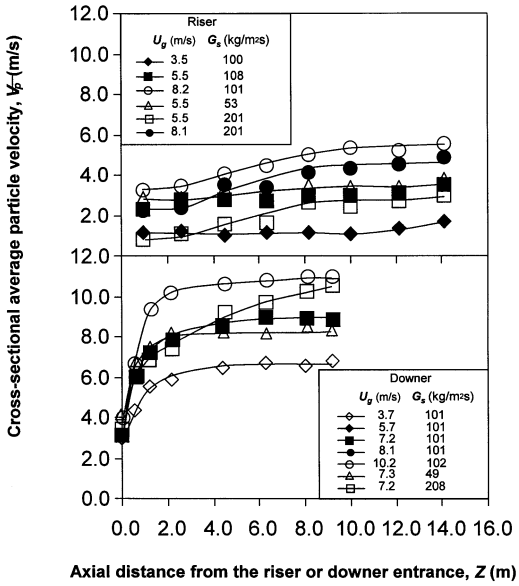

Figure 8. Axial profiles of cross-sectional average particle velocity along the riser and downer at various operating conditions.

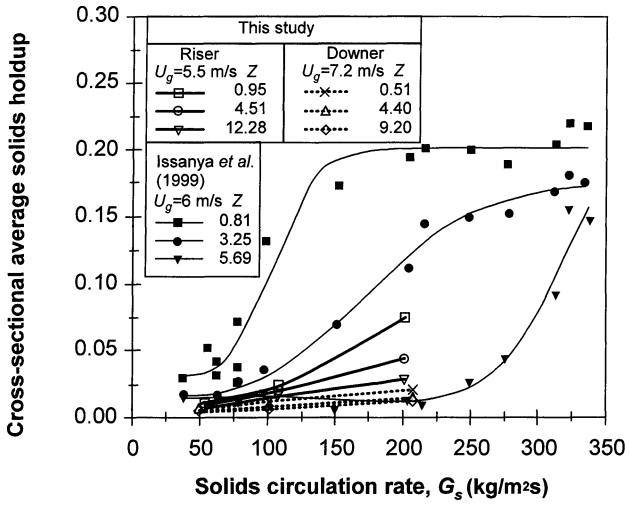

Figure 9. Cross-sectional average solids holdup at various heights along the riser and downer as a function of solids circulation rate.

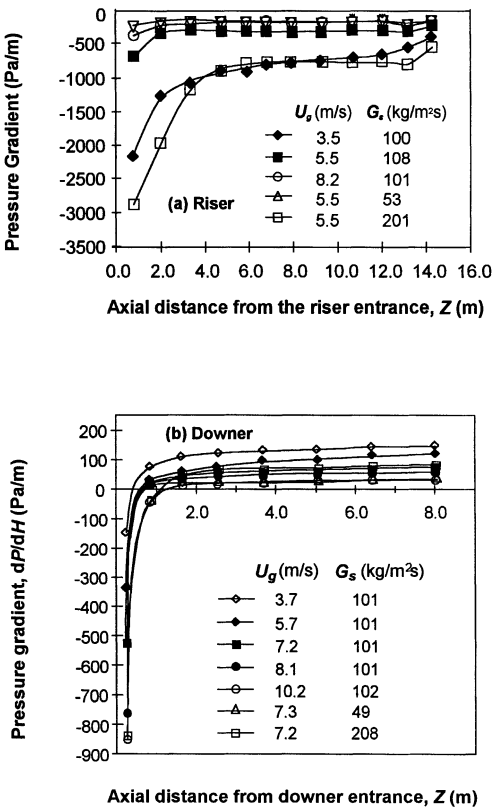

Figure 10. Axial profiles of pressure gradient along the riser and downer at various operating conditions.

of particle acceleration (LOA) in the downer is between 1 and 4 m. At some extreme conditions, such as $G_s = 200$ kg/m^2·s with $U_g \geq 7.2$ m/s, the LOA becomes longer than the length of the downer (9.3 m). For most of the operating conditions tested, the length of particle acceleration (LOA) in the riser is between 2 and 8 m. At some extreme conditions, such as $U_g = 3.5$ m/s with $G_s \geq 100$ kg/m^2·s, the LOA becomes longer than the length of the riser (15 m).

Both an increase in G_s and an increase in U_g extend LOA in the downer. Furthermore, LOA in the downer is very sensitive to the change in G_s, but less sensitive to U_g, probably because solids acceleration is primarily due to gravity. In the riser, an increase in G_s extends LOA, but an increase in U_g shortens LOA. Unlike the downer, the LOA in the riser is sensitive to both changes in G_s and U_g.

As described above, the nozzle type gas distributor used in this study provides a very high acceleration to the particles at the entrance section of the riser, so that a dense phase was not observed for all the conditions tested. However, for other distributor designs, a dense phase can be present at the riser bottom and an S-shaped axial solids holdup profile will be formed. Figure 9 illustrates the experimental results obtained by Issangya et al. (1999) in a 76.2 mm riser, as well as the results in the riser and the downer in this study. It can be seen that in the riser of Issangya et al. (1999) at a U_g of 6.0 m/s a dense phase starts to form at the bottom when G_s exceeds about 75 kg/m^2·s while the top remains dilute until G_s exceeds 275 kg/m^2·s. Thus, when G_s is between these two values, the riser in their study possesses three different axial sections: the dense section at the bottom, the dilute section at the top, and the transition section in the middle where particles are accelerated. In the riser of this study, the difference in solids holdup between the top and the bottom is not obvious even though the three profiles split apart somewhat when G_s reaches about 200 kg/m2s. In the downer of this study, the difference between the downer top and the downer bottom is even less significant compared to the riser. Obviously, it is almost impossible to form a dense phase in the downer because of the gravitational acceleration imposed to the particles.

Pressure Gradients in the Riser and the Downer. Figure 10 shows the axial profiles of pressure gradient measured in the riser and the downer. In the riser, the pressure gradient is always negative because the gas phase loses pressure head to accelerate and to suspend the particles. Therefore, the particles move from high pressure to low pressure in the riser. The absolute values of pressure gradient decrease monotonically with increasing distance from the riser entrance and then gradually approach a constant value. Due to the nozzle type design of the gas distributor, no dense phase is observed at the bottom of the riser so that at the entrance section, a constant pressure gradient is also not observed in this study. Thus, the two-section structure in the axial direction of a riser can also be recognized from the pressure gradient profile: the acceleration section with a decreasing pressure gradient, and the dilute phase section (constant velocity section) with a low constant pressure gradient.

In the downer, the pressure gradient increases monotonically with increasing distance from the downer entrance and then gradually approaches a constant value. It starts with a large negative value, and then becomes positive before approaching the constant value. The particles move from high

pressure to low pressure in the first acceleration section and then move from low pressure to high pressure in the second acceleration section and the constant velocity section. The three-section structure in the axial direction in the downer is reflected by the pressure gradient profiles: the first acceleration section with a negative pressure gradient, the second acceleration section with a positive and increasing pressure gradient, and the constant velocity section with a constant pressure gradient (Wang et al., 1992).

From the above experimental results and discussion on the axial flow structures in the two reactors, it can be summarized that due to the opposite effects of gravity on the particle phases in the riser and the downer, the axial flow structure in the downer significantly differs from that in the riser. First of all, the particles in the acceleration sections of the downer acquire higher acceleration compared to the particles in the riser under comparable operating conditions. In this study, the results show that LOA in the downer is generally between 1 and 4 m, while LOA in the riser is mostly between 2 and 8 m. Secondly, the particles in the downer travel faster than the gas in the second acceleration section and the constant velocity section while the particle velocity in the riser is always lower than the gas velocity. Furthermore, due to the higher acceleration in the downer, the particle velocity in the first acceleration section is also higher than that at the entrance of the riser. The higher particle velocity in the downer leads to a lower solids holdup. Thirdly, in the downer, both the increases in G_s and U_g extend LOA, while in the riser, the increase in G_s extends LOA but the increase in U_g shortens it. Finally, because a dense phase normally cannot be formed in the downer, the overall axial nonuniformity in terms of solids holdup and particle velocity is very small compared to that in the riser.

Flow regimes in the gas-solids systems

The fast fluidization, as well as the dense phase and dilute phase transports, with gas and solids cocurrently flowing upward, have received extensive research over past two decades. In recent years, much attention has also been given to the gas-solids cocurrent downflow fluidization and systematical experimental investigations have been carried out in this laboratory. However, there is not a regime map which covers both upflow and downflow systems. With the results from the downer and the riser in this study and from many previous studies in risers (Bai et al., 1991b; Takeuchi et al., 1986), a regime map is proposed as shown in Figure 11. In this figure, as originally proposed by Zhu (1999), the fluidization regimes are mapped against the operating conditions (the superficial gas velocity and the solids circulation rate).

The first quadrant of this new regime map is for gas and solids upflow systems. Mainly determined by the superficial gas velocity, a fluidized bed with upflow gas phase can be operated in different flow regimes ranging from conventional fluidization (bubbling and turbulent fluidization) to fast fluidization and then to dense phase and dilute phase transport (Bai et al., 1991b). There have been some contentions on whether the "dense-phase transport" should be considered a separate regime from the fast fluidization regime and where the boundary lies between these two regimes. However, if the net downward solids flux near the wall and the distinctive

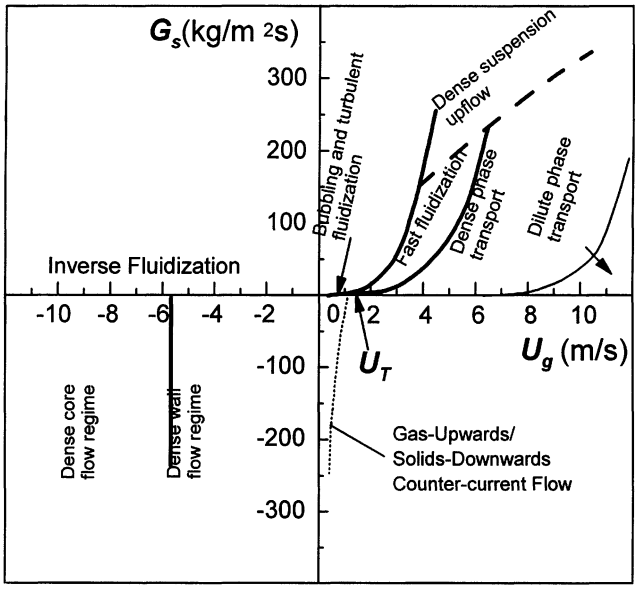

Figure 11. New regime map for the gas-solids fluidization system (for FCC particles).

bed density difference between the top and the bottom of the riser are taken as the distinguishing features of the fast fluidization, the regime divisions for the cocurrent upflowing gas-solids system can thus be made as shown in Figure 11. Grace et al. (1999) proposed a dense suspension upflow regime that differs from fast fluidization and pneumatic transport. This regime shows no net downward flux at the wall and the high solids holdup ($\epsilon_s > 0.1$) is distributed uniformly in the axial direction due to the expansion of the dense section at high solids circulation rate. On the other hand, the dense-phase transport regime has the similar features described above. The only difference is that in this regime, the uniform distribution of low solids holdup in the axial direction comes from the expansion of the dilute-phase section at lower solids circulation rate relative to the dense suspension upflow regime (or at higher superficial gas velocity relative to the fast fluidization regime). Therefore, the discrepancy that lies between the "dense suspension upflow" and the "dense-phase transport" could only be the overall difference of solids holdup in the riser between the two "regimes".

All the possible regimes in the riser, from fast fluidization to dilute-phase transport, have a common feature: the nonuniform radial distributions of particle velocity and solids holdup, with the highest particle velocity at the center and the highest solids holdup at the wall.

Shown in the third quadrant, the gas-solids cocurrent downflow system (downer) can also be operated in different regimes as proposed by Zhang (1999). Again, mainly depending upon the superficial gas velocity, two different flow regimes can be obtained: the "dense core flow regime" with a superficial gas velocity higher than about 5.7 m/s and the "dense wall flow regime" with a superficial gas velocity lower than about 5.7 m/s. These terminologies for the two regimes describe the radial distributions of the gas-solids flow across the crosssection of the downer. Being around 5.7 m/s, the

transition point of superficial gas velocity seems not to be affected by the solids circulation rate.

In the gas-solids downer system, no matter which regime the downer is operated in, the macro radial and axial uniformities of particle velocity and solids holdup are significantly higher than those found in the riser, as discussed earlier. Also, the microflow structure, reflected by the intermittency index, is always more uniform than that in the riser. These properties of the downer would ensure a higher gas and solids contact efficiency and a higher product selectivity. For the potential applications of the downer reactor (such as FCC reaction), it would be mostly operated at high gas/solids loading ratios which make the downer reactor operate in the relatively less uniform dense core regime. Nonetheless, the overall uniformities throughout the downer ensure that the downer is very advantageous over the riser.

Operation in the second quadrant is also possible in principle with downflowing gas entrains solids cocurrently downwards, when the particles are lighter than the gas. This so-called inverse fluidization has been realized with liquid-solids systems where lighter particles than the liquid are easier to find (Fan et al., 1982; Karamanev and Nikolov, 1992). Operation in the fourth quadrant involves particles dripping down through upward gas flow and has not been given too much attention. The preliminary work by Luo et al. (2000) shows that such operation is possible over a wide range of G_s, but a narrow range of U_g. Such gas-upwards/solids-downwards countercurrent flow also leads to high-solids holdup, something that is difficult to achieve for the downer operations in the third quadrant.

Existing limitations of the downer

Having presented the many advantages of the downer compared to the riser, it is also necessary to point out the limitations of the downer. The main limitation of the downer is the very low solids holdup, associated with which comes the somewhat lower heat-transfer coefficient in the downer (Ma and Zhu, 1999, 2000). The low solids holdup results from the high particle velocity in the downer and the low capacity of the solids feeding. For example, in an FCC downer system operating at 8 m/s, the "equilibrium" particle velocity in the developed region is about 9 m/s. Assuming that the particle velocity entering the top has already attained its terminal velocity (~ 0.18 m/s), the highest solids holdup in the developed region is less than 1% ($= 0.18/9 \times (0.5)$ and the highest solids circulation rate is less than 135 kg/m$^2\cdot$s ($= 0.18 \times 0.5 \times 1{,}500$). Clearly, solids feeding becomes the limitation. In the present study, particles have already been accelerated somewhat in the solids distributor tubes so that we can achieve higher (but not much than) than solids holdup and circulation rate. To overcome this limitation, Liu et al. (2000) have studied a high-density downer where a large funnel feeder is used to preaccelerate the solids before feeding into the downer. Solids holdup up to 10–12% and solids circulation rates up to 400 kg/m$^2\cdot$s have been achieved for FCC particles in their specially designed downer column.

Conclusions

The radial flow structure in the downer, in terms of the radial distributions of solids holdup and particle velocity, is much more uniform than that in the riser. The radial nonuniformity indices (RNIs) of solids holdup and particle velocity in the downer are normally several times lower than that in the riser under comparable operating conditions. The local particle velocity in the downer is always higher compared to that under similar operating conditions in the riser, and, therefore, the local solids holdup in the downer is always lower than that in the riser. The core-annulus flow structures exist in both the riser and the downer. In the downer, the solids holdup in the annulus can be either higher or lower than that in the core, depending upon which regime it is operated in. While in the riser, the solids holdup in the annulus is always higher than that in the core. In both reactors, the particle velocity in the core is always higher than that in the annulus. However, in the fully developed zone of the downer, the radial profile of particle velocity is very flat in the large core region, while the profile in the riser decrease monotonically from the center toward the wall in the fully developed zone. Due to the uniform radial flow structure in the downer, it is favorable to a narrow RTD.

The microflow structure in the downer is also more uniform than that in the riser. The intermittency indices in the core regions of the two reactors are comparable to each other. In the annular region, however, the solids particles in the downer are in a more particulate form, while in the riser, they tend to be in a more aggregated form in this region.

The length of flow development in the annular region of the downer is comparable to that of the riser. In the core region of the downer, LOD is always longer than that of the riser. The total LOD in the downer, however, is comparable to that of the riser.

The axial flow structure in the downer is also more uniform than that in the riser, because, normally, no dense phase section can be formed in the downer. Compared to the riser, the solids holdup in the downer is significantly lower than that in the riser due to the higher particle velocity in the downer. The higher particle acceleration in the downer leads to a shorter LOA.

A new flow regime map is proposed to present all flow regimes in the upflow and downflow systems. The first quadrant of this regime map shows that a fluidized bed with upflow gas phase can be operated in different flow regimes ranging from conventional fluidization (bubbling and turbulent fluidization) to fast fluidization and then to dense phase and dilute phase transport, mainly depending on the superficial gas velocity. When the solids circulation rate is high enough, it enters the dense suspension upflow regime. In the third quadrant, the gas-solids cocurrent downflow system (downer) can be operated in the dense core flow regime and the dense wall flow regime. The transition point between these two regimes is about 5.7 m/s for FCC particles.

The key properties of the downer (uniform macro radial and axial-flow structure, uniform microflow structure) make it an excellent candidate for industrial applications where high-gas and solids contact efficiency, high-product selectivity and short-reaction time are highly needed.

Notation

G_s = solids circulation rate, kg/m$^2\cdot$s
LOA = length of particle acceleration obtained from the axial

solids concentration profiles or from the axial particle velocity profiles, m
LOD = comprehensive length of radial flow development, m
dP/dZ = pressure gradient, Pa/m
r/R = normalized radial distance from the center of the downer or riser
RNI(V_p) = radial nonuniformity index for V_p, normalized standard deviation of the cross-sectional average particle velocity
RNI(ϵ_s) = radial nonuniformity index for ϵ_s, normalized standard deviation of the cross-sectional average solids holdup
RTD = particle residence time distribution
U_g = superficial gas velocity, m/s
U_T = terminal velocity, of single particle, m/s
V_p = local particle velocity, m/s
$\bar{V}_p$ = cross-sectional average particle velocity, m/s
Z = distance from the downer or riser entrance, m

Greek letters

γ = intermittency index
ϵ_s = local solids holdup
$\bar{\epsilon}_s$ = cross-sectional average solids holdup

Literature Cited

Bai, D-R., Y. Jin, Z-Q. Yu, and N-J. Gan, "Radial Profiles of Local Solid Concentration and Velocity in a Concurrent Downflow Fast Fluidized Bed," P. Basu, M. Horio, and M. Hasatani, eds., *Circulating Fluidized Bed Technology III*, Pergamon Press, Toronto, pp. 157–162 (1991a).

Bai, D-R., Y. Jin, and Z-Q. Yu, "Circulating Fluidization," (in Chinese), *Chem. React. Eng. Technol.,* **7**(2), 202 (1991b).

Bassi, A. B., C. L. Briens, and M. A. Bergougnou, "Short Contact Time Fluidized Reactors (SCTFRs)," *Circulating Fluidized Bed Technology IV*, A. A. Avidan, ed., AIChE, New York, pp. 15–19 (1994).

Berruti, F., J. Chaouki, L. Godfroy, R. S. Pugsley, and G. S. Patience, "Hydrodynamics of Circulating Fluidized Risers: A Review," *Can. J. Chem. Eng.*, **73**, 579 (1995).

Brereton, C. M. H., and J. R. Grace, "Microstructural Aspects of the Behaviour of Circulating Fluidized Beds," *Chem. Eng. Sci.*, **48**, 2565 (1993).

Cao, C., and H. Weinstein, "Characterization of Downflowing High Velocity Fluidized Beds," *Advanced Technologies for Particle Processing (Extended abstracts)*, AIChE Meeting, Miami Beach, FL, 38 (Nov. 1998).

Fan, L.-S., K. Muroyama, and S.-H. Chern, "Hydrodynamic Characteristics of Inverse Fluidization in Liquid-Solid and Gas-Liquid-Solid Systems," *Chem. Eng. J.*, **24**, 143 (1982).

Grace, J. R., "High Velocity Fluidized Bed Reactors," *Chem. Eng. Sci.*, **45**, 1953 (1990).

Grace, J. R., A. S. Issangya, D-R. Bai, and X-T. Bi, "Situating the High-Density Circulating Fluidized Bed," *AIChE J.*, **45**, 2108 (1999).

Hartge, E-U., Y. Li, and J. Werther, "Flow Structures in Fast Fluidized Beds," *Fluidization V*, K. Ostergaard and Sorensen, eds., Engineering Foundation, New York, pp.165–180 (1986).

Hartge, E-U., D. Rensner, and J. Werther, "Solids Concentration and Velocity Patterns in Circulating Fluidized Beds," P. Basu and J. F. Large, eds., *Circulating Fluidized Bed Technology II*, P. Basu and J. F. Large, eds., Pergamon Press, Toronto, pp. 165–180 (1988).

Herb, B., K. Tuzla, and J. C. Chen, "Distribution of Solids Concentrations in Circulating Fluidized Bed," J. R. Grace, L. W. Shemilt, and M. A. Bergougnou, eds., *Fluidization VI*, Engineering Foundation, New York, pp. 65–72 (1989).

Herbert, P. M., T. A. Gauthier, C. L. Briens, and M. A. Bergougnou, "Flow Study of a 0.05m Diameter Downflow Circulating Fluidized Bed," *Powder Technol.*, **96**, 255 (1998).

Issangya, A. S., D. Bai, H. T. Bi, K. S. Lim, J. Zhu, and J. R. Grace, "Suspension Densities in a High-Density Circulating Fluidized Bed Riser," *Chem. Eng. Sci.*, **54**, 5451 (1999).

Jiao, S-Y., J-X. Zhu, M. A. Bergougnou, M. Ikura, and M. Stanciulescu,"Investigation and Modelling of the Thermal Cracking of Waste Plastics Derived Oil in a Downer Reactor," *Trans IChemE.*, **76**(B), 319 (1998).

Johnston, P. M., H. I. de Lasa, and J.-X. Zhu, "Axial Flow Structure in the Entrance Region of a Downflow Fluidized Bed—Effects of the Distributor Design," *Chem. Eng. Sci.*, **54**, 2161 (1999).

Karamanev, D. G., and L. N. Nikolov, "Bed Expansion of Liquid-Solid Inverse Fluidization," *AIChE J.*, **38**, 1916 (1992).

Lehner, P., and K. E. Wirth, "Effects of the Gas Solids Distributor on the Local and Overall Solids Distribution in a Downer Reactor," *Can. J. Chem. Eng.*, **77**, 199 (1999).

Li, J., and M. Kwauk, "The Dynamic of Fast Fluidization," *Fluidization,* J. R. Grace and J. M. Matsen, eds., Plenum Press, New York, pp. 537–544 (1980).

Liu, W-D., K-B. Luo, J-X Zhu, and J. M. Beeckmans, "Characterization of High Density Gas-Solids Downflow Fluidized Beds," *Powder Technol.*, in press (2000).

Luo, K-B., W-D. Liu, J-X Zhu, and J. M. Beeckmans, "Characterization of Gas Upward-Solids Downward Counter-Current Fluidized Flow," *Powder Technol.*, in press (2000).

Ma, Y., and J-X. Zhu, "Experimental Study of Heat Transfer in a Co-Current Downflow Fluidized Bed (Downer)," *Chem. Eng. Sci.*, **54**, 41 (1999).

Ma, Y., and J-X. Zhu, "Heat Transfer between Gas-Solids Suspensions and Immersed Surface in an Upflow Fluidized Bed (Riser)," *Chem. Eng. Sci.*, **55**, 981 (2000).

Mori, S., D. Liu, K. Kato, and E. Kobayashi, "Flow Regimes and Critical Velocity in a Circulating Fluidized Bed," *Powder Technol.*, **70**, 223 (1992).

Takeuchi, H., T. Hirama, T. Chiba, J. Biswas, and L. S. Leung, "A Qualitative Definition and Flow Regime Diagram for Fast Fluidization," *Powder Technol.*, **47**, 195 (1986).

Wang, Z., D. Bai, and Y. Jin, "Hydrodynamics of Cocurrent Downflow Circulating Fluidized Bed (CDCFB)," *Powder Technol.*, **70**, 271 (1992).

Wei, F., Z. Wang, Y. Jin, Z. Yu, and W. Chen, "Lateral and Axial Solids Dispersion in a Cocurrent Downflow Circulating Fluidized Bed," *Powder Technol.*, **81**, 25 (1994).

Wei, F., and J.-X. Zhu, "Effect of Flow Direction on the Solids Mixing in Gas-Solids Upflow and Downflow Systems," *Chem. Eng. J.*, **64**, 345 (1996).

Wirth, K.-E. and T. Schiewe, "Flow Structures in a Downer Reactor," L.-S. Fan and T. M. Knowlton, eds., *Fluidization IX*, Engineering Foundation, New York, pp. 253–260, (1998).

Yang, Y.-L., Y. Jin, Z.-Q. Yu, Z.-W. Wang, and D.-R. Bai, "The Radial Distribution of Local Particle Velocity in a Dilute Circulating Fluidized Bed," P. Basu, M. Horio, and M. Hasatani, eds., *Circulating Fluidized Bed Technology III*, Pergamon Press, Toronto, pp. 201–206, (1991).

Zhang, H., P. M. Johnston, J.-X. Zhu, H. I. de Lasa, and M. A. Bergougnou, "A Novel Calibration Procedure for a Fibre Optic Concentration Probe," *Powder Technol.*, **100**, 260 (1998).

Zhang, H., "Hydrodynamics of a Gas-Solids Downflow Fluidized Bed Reactor," PhD Diss., University of Western Ontario, London, Canada (1999).

Zhang, H., J-X. Zhu, and M. A. Bergougnou, "Hydrodynamics in Downflow Fluidized Beds (1): Solids Concentration Profiles and Pressure Gradient Distributions," *Chem. Eng. Sci.*, **54**, 5461 (1999).

Zhang, H., and J-X. Zhu, "Hydrodynamics in Downflow Fluidized Beds (2): Particle Velocity and Solids Flux Profiles," *Chem. Eng. Sci.*, **55**, 4367 (2000).

Zhang, W., Y. Tung, and J. E. Johnsson, "Radial Voidage Profiles in Fast Fluidized Beds of Different Diameters," *Chem. Eng. Sci.*, **46**, 3045 (1991).

Zhou, J., J. R. Grace, S. Z. Qin, C. Brereton, C. J. Lim, and J. Zhu, "Voidage Profiles in a Circulating Fluidized Bed of Square Cross-Section," *Chem. Eng. Sci.*, **49**, 3217 (1994).

Zhu, J.-X., Z-Q. Yu, Y. Jin, J. R. Grace, and A. Issangya, "Cocurrent Downflow Circulating Fluidized Bed (Downer) Reactors—A State of the Art Review," *Can. J. Chem. Eng.*, **73**, 662 (1995).

Zhu, J-X., and F. Wei, "Recent Developments of Downer Reactors

and Other Types of Short Contact Reactors," J. F. Large and C. Laguerie, eds., *Fluidization VIII*, Engineering Foundation, New York, pp. 501–510 (1996).
Zhu, J-X., "Expansion of the Fluidization Concept: Upflow, Downflow and Counter Flow," Syncrude Innovation Award Plenary Lecture, *49th Annual Can. Society of Chem. Eng. Conf.*, Saskatoon, Saskatchewan, Canada (Oct. 3–6, 1999).
Zhu, J.-X., and S. V. Manyele, S. V., "Radial Non-Uniformity Index (RNI) in Fluidized Beds and other Multiphase Flow Systems," *Can. J. Chem. Eng.*, **79**, 279 (2001).
Zhu, J-X., G-Z. Li, S-Z. Qin, F-Y. Li, H. Zhang, and Y-L. Yang, "Direct Measurements of Particle Velocities in Gas-Solids Suspension Flow Using a Novel 5-Fiber Optical Probe," *Powder Technol.*, **115**, 184 (2001).

Manuscript received Jan. 12, 2000, and revision received Mar. 20, 2001.